Characterization of an Integrable Single-Crystalline 3-D Tactile Sensor

Gábor Vásárhelyi, *Student Member, IEEE*, Mária Ádám, Éva Vázsonyi, Zsolt Vízváry, Attila Kis, István Bársony, *Member, IEEE*, and Csaba Dücsõ

Abstract—**Porous-Si-micromachining technique was used for the formation of single-crystalline force-sensor elements, capable of resolving the three vector components of the loading force. Similar structures presented so far are created from deposited polycrystalline Si resistors embedded in multilayered SiO_2/Si_3N_4 membranes, using surface micromachining technique for a cavity formation. In this paper, the authors implanted four piezoresistors in an n-type-perforated membrane, having their reference pairs on the substrate in order to form four half bridges for the transduction of the mechanical stress. They successfully combined the HF-based porous-Si process with conventional doping and Al metallization, thereby offering the possibility of integration with readout and amplifying electronics. The $300 \times 300 ~\mu m^2$ membrane size allows for the formation of large tactile arrays using single-crystalline-sensing elements of superior mechanical properties. They used the finite-element method for modeling the stress distribution in the sensor, and verified the results with real measurements. Finally, they covered the sensors with different elastic silicon–rubber layers, and measured the sensor's altered properties. They used continuum mechanics to describe the behavior of the rubber layer.**

Index Terms—**Porous-Si micromachining, tactile sensors, three-dimensional (3-D) force sensors.**

I. INTRODUCTION

A LARGE variety of silicon-based tactile sensors has been developed for robotic applications to measure the contact stress by an array of pressure-sensing elements. Robot fingers, however, must perform complex grasping and manipulating tasks influenced by three-dimensional (3-D) forces.

The known sensor designs are composed of a central shuttle plane either as a full membrane [1] or suspended by four bridges above a micromachined cavity [2]. The orientation of the bridges and the shape of the central platform are determined by the fabrication process. Anisotropic etching [1] results in a membrane-edge orientation of $\langle 110 \rangle$. In the bridge-suspended
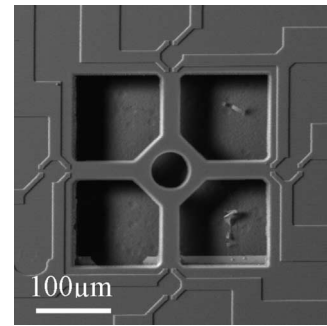
Fig. 1. Scanning electron micrograph of the sensor structure. Characteristic dimensions: bridge $80 \times 32 \times 10 ~\mu m^3$, plate $100 \times 100 \times 10 ~\mu m^3$, hole 50-$\mu$m diameter, cavity depth cc. 35 μm.

membrane approach [2], the piezoresistors were formed out of polycrystalline silicon embedded in deposited silicon nitride layers. The membrane was released by front-side alkaline etching of the single-crystalline silicon underneath. Although the process is CMOS compatible, the structure suffers from the limited sensitivity and mechanical stability of the multilayered membrane.

In this paper, we will present the construction of a monocrystalline silicon tactile-sensing element, unifying the advantages of both the above approaches. The single-crystalline silicon as a structural material provides excellent and controllable mechanical properties in all directions. Moreover, the manufacturing process can be integrated into the microcircuit technology. The main advantage of the proposed method lies in the freedom provided by the use of the single-side porous-silicon micromachining for the formation of the suspended n-type single crystal membrane. In this way, there is no orientation restriction in the membrane design whatsoever. Moreover, it also facilitates the formation of the optimum p$^+$ piezoresistors.

Another important issue in tactile sensor design is the elastic covering. According to [3] and [4], the rubber layer glued on top of a sensor acts as an information-coding layer and essentially changes the sensor's characteristics. In this paper, we propose different methods for covering the sensors and changing their properties to achieve robust but sensitive functioning. We also introduce a new design for enhancing lateral forces, which is of great importance in robotic grasping applications.

II. SENSOR DESIGN

The single-crystalline-sensory element (Fig. 1) consists of a central plate, suspended by four bridges over an etched cavity.
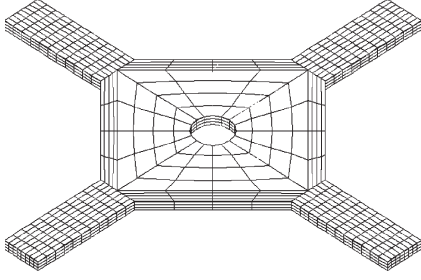
Fig. 2. Three-dimensional meshing of the sensor, used in the FEM calculations. We built up the model with eight-noded brick elements.

Because the central part of the membrane is more rigid than the bridges, they are the only parts that deform under load. Each of the four bridges includes a p^+ piezoresistor that is used as an independent strain gauge. The center hole of the membrane allows for the possible insertion of a load-transmitting element.

A. Mechanical Modeling

We designed the geometry of the structure with the finite-element method (FEM) using the Cosmos/M 2.0 package. The aim was to find the optimum feasible sizes and to reach the highest sensitivity without deteriorating the sensor. The working interval was defined in the force range of 0.1–10 mN.

The 3-D finite element model was built up using eight-noded brick elements (Fig. 2).

In the model, a protrusion in the central hole of the membrane receives the load and leads to a magnification of the lateral-force components. We considered three different load cases, normal force, and shear force with different directions. The three basic loads are:

1) normal force normal to the plane of the membrane (F_z);
2) shear force in direction x parallel to the suspending beams (F_x);
3) shear force attacking at $45°$ with respect to both x- and y-directions (F_{xy}).

The sensitivity of a p-type (110) oriented piezoresistor on a $\langle 100 \rangle$ chip can be calculated by the following [5]:

$$\frac{\Delta R}{R} = \frac{\Delta V}{V} \cong \frac{\pi_{44}}{2} \cdot (\sigma_l - \sigma_t) \quad (1)$$

where R is the zero stress resistance, ΔR is the resistance change when stress is present, π_{44} is the dominant piezoresistive coefficient of the material (π_{11} and π_{12} are relatively small, hence they are neglected), σ_l and σ_t are the longitudinal and transversal stress components, respectively.

The stress must be as high as possible at the location of the piezoresistors, on the other hand it must never exceed the yield stress, which has a well-known value for the single-crystalline silicon (250 MPa). Since reliable yield stress values for silicon nitride are hard to find, we chose the value of 250 MPa to limit the stresses in the sensor. We used the von Mises equivalent stress (2) to have a general estimate value of the stress field

$$\sigma_{vM} = \sqrt{\frac{1}{2} \left[(\sigma_1 - \sigma_2)^2 + (\sigma_2 - \sigma_3)^2 + (\sigma_3 - \sigma_1)^2 \right]}. \quad (2)$$

TABLE I
CALCULATED STRESSES (MPa) AND SENSITIVITY AT THE UPPER END OF THE FORCE INTERVAL (10 mN) IN THE DIFFERENT LOAD CASES, FOR A GEOMETRY GIVEN IN FIG. 1

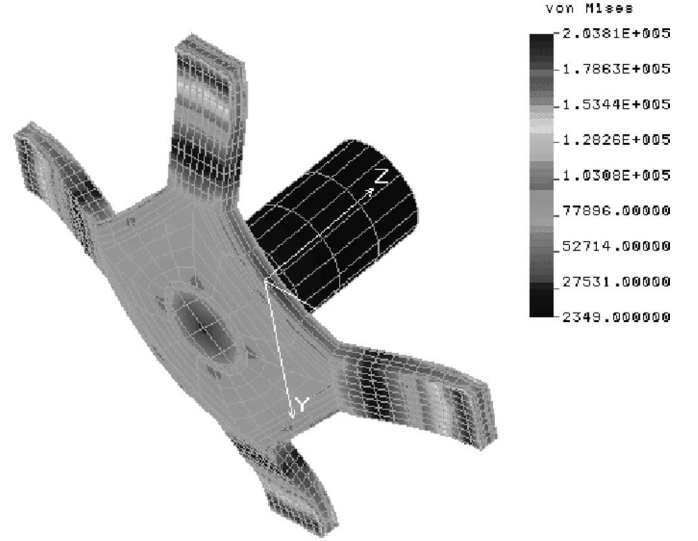| Load	σ_{vM}	σ_l	σ_t	$\Delta R/R$
F_z	203.8	−203.5	−38.2	−0.114
F_x	293.2	290	55.6	0.162
F_{xy}	269.9	205	39.3	0.114

Fig. 3. Stress field (σ_{vM}) of the sensor in response to 10-mN force applied in the z-direction.

The results—calculated for a geometry shown in Fig. 1—are listed in Table I. The used materials are assumed to be homogeneous, isotropic, and linearly elastic, therefore the obtained stresses are proportional to the loads.

The stress field (σ_{vM}) for load F_z (10-mN force applied normally to the membrane) is presented in Fig. 3. More detailed description about the FEM modeling can be found in [6].

III. EXPERIMENTAL

A. Wafer Processing

Standard p-type 10–15 $\Omega \cdot$ cm (100) Si wafers were selectively doped with phosphorus by ion implantation. After annealing, we obtained an n-type region, resulting in a total membrane thickness of 10 μm. We prepared the p^+ piezoresistors in this layer by boron implantation followed by silicon nitride masking pattern on the front side and depositing an aluminum layer on the back. Then, we performed an 800-s electrochemical etching process in a galvanostatic regime, using a hydrofluoric acid and ethanol mixture at 7:3 ratio with a current density of 60 mA/cm^2. The resulting porous layer was 34–36 μm in thickness. In order to maintain the integrity of the suspended membranes, we dissolved the porous-Si layer from the individually cut chips.

B. Sensor Packaging

After processing, we die bonded the chips onto a printed circuit board (PCB). We made electrical connections between
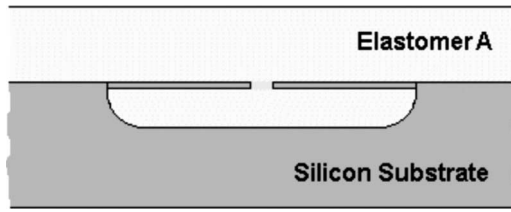
Fig. 4. Schematic cross section of a sensing element covered by silicon rubber.

the PCB and the sensor array using a standard Al wire ultrasonic technique. Then, we coated the wire bond connections and the wires with a two-component epoxy[1] to prevent mechanical damage.

We processed the active sensing regions in two different ways.

1) In the first version, we covered the sensing elements with elastic silicon rubber (Fig. 4). The rubber (Elastomer A)[2] infiltrates the cavity and also forms a coating with the designed thickness on the membrane and the suspensions. The sensor's sensitivity and protection therefore depends on the thickness and the hardness of the layer. We set these properties so that they resemble the "coverage" of the human finger.

2) In the second version packaging design, we built a small plastic rod in the middle of the sensory element to enhance shear load transmission.

This load transmitting element, made of epoxy,[3] protrudes through the center hole of the membrane and sits on the elastic epoxy[4] layer, which fills the cavity to the half of its depth.

After, we prefabricated a layer of Elastomer A (with a thickness of 50–500 μm) and glued it to the top of the rod with Elastomer B.[5] For precise positioning, we temporarily placed a spacer tool outside the active area. During this procedure, the silicon rubber filled up the remainder of the cavity. In the final step, we injected viscous silicon rubber (of type Elastomer A) into the space between the top elastomer and the Si surface around the taxel, thereby providing robust compact coverage. A scheme of the cross section of the complete sensor is presented in Fig. 5, while a photograph of the load transferring structure is shown in Fig. 6.

Before the functional testing of the differently covered sensors, we also investigated the response characteristics of the bare elements as a reference.

C. Measuring Setup

The experimental setup consisted of a loading instrument and signal measuring, data acquisition, and processing systems.

In the mechanical test station, we fixed the sensor on a precision x–y table that could be tilted around the x-axis. We used an electromagnetic force transducer mounted on a

[1] Araldite D, Vantico Ltd.
[2] OXAM DC, T-Silox Ltd.
[3] Araldite 2014, Vantico Ltd.
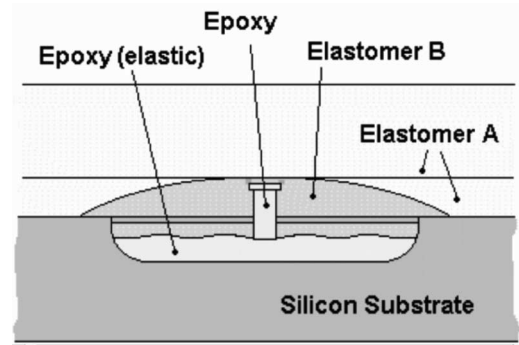[4] Araldite DY022, CIBA.
[5] ELASTOSIL E41 Wacker-Chemie GmbH.

Fig. 5. Cross section of the sensing structure after the completion of the covering process. In this version, a load transmitting rigid bump is attached to the membrane to enhance shear sensitivity.
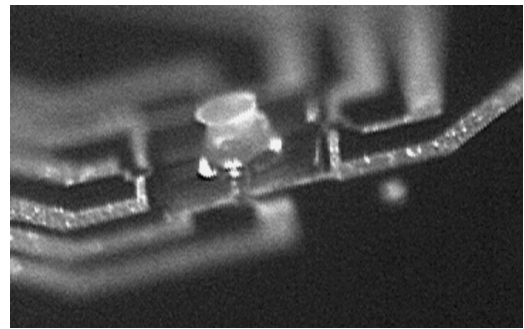

Fig. 6. Photograph of a single taxel with a plastic rod glued on top. This unit increases the sensor's sensitivity to shear forces.

movable stage to apply load in the z-direction. We adjusted the orientation of the force by altering the tilt and rotating the sensor in the plane of the x–y table. We observed the accurate position of the tip of the loading tool through a stereo microscope.

The piezoresistors and their reference pairs were arranged in a half-bridge configuration in the design, providing a direct voltage reading proportional to the strain. The bias voltage was 5 V in all the cases.

In the first generation setup, we measured the node voltages with a Keithley 617 Programmable Electrometer across a Keithley 705 Scanner at each node. We used the LabView 6.0 package for control and data acquisition via the IEEE-488 bus.

Finally, we developed a linear amplification stage and used an Advantech PCI 1713 A/D converter card to achieve real-time measurement speed, necessary for high-precision experiments and further applications.

IV. MECHANICAL TESTING

Mechanical testing requires a lot of patience and care. The loading tip should be adjusted precisely in all three dimensions without overloading the bridges. Since the diameter of the tip is small, high local pressure values can easily be achieved. The SEM cross section of the result of a "nonprecise attempt" on a noncovered structure is shown in Fig. 7.

We experimented with three different sensor types. First, we tested the bare Si membrane without any protective layer, then we measured the responses of sensors with elastic covers
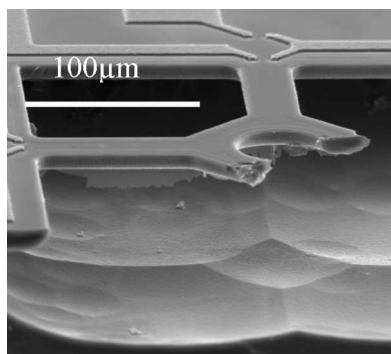
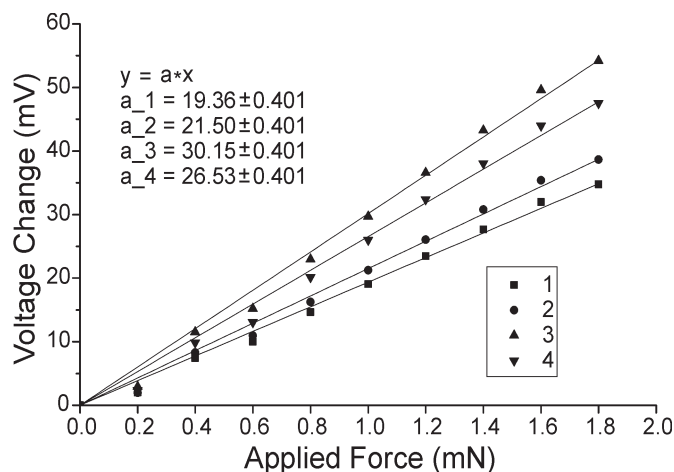Fig. 7.   Scanning electron micrograph of a cleaved sensing element.

Fig. 8.   Linear response of the four piezoresistive bridges of one sensing element. The difference in the slopes is the result of the indefinite positioning of the loading tip.

Fig. 9.   Exponential-like response of the four bridges of one sensory element. Indentation tip diameter is 100 μm. Equivalent pressure values are calculated—the nonlinear response in the rubber's elasticity is the result of the high local pressure.

of different thickness, and finally we analyzed membranes with load transferring rigid rods and silicon–rubber protection. For all three cases, the main difficulty of the measurements was in the very fine adjustment of the indentation position and weight. The three sensor types required different loading ranges, and indentation shapes and sizes. Results for each case are summarized below.

A. Bare Si Membrane—Characterization of the Si Element—Linear Response

First, we applied normal load in the range of 0–2 mN to the center of the bare membrane surface. The indentation tip had a round flat surface with a diameter of 100 μm. The predicted linear response of the piezoresistive elements [6] was verified by the loading tests. Although we achieved linear response with small noise in every single measurement (Fig. 8), the uncertainty in the fine positioning of typically ± 30 μm resulted in a relatively large variation of the slopes of the functions. Unfortunately, the rigid and undefined contact between the membrane and the needle prevented the total repeatability of the measurements. Nevertheless, the calculated sensitivity from experimental data (4–6 mV/mN/V) is close to the FEM result for the same sensor (2.9 mV/mN/V).
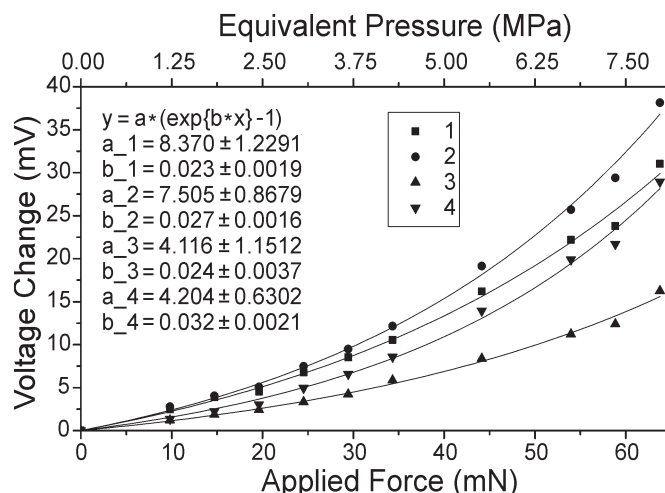
B. Characterization of the Sensor With Silicon Rubber on Top

In these experiments, the aim was to check the linearity of the response of the sensing element versus the load magnitude. However, this only depends on the linearity of the load transfer to the membrane, since the piezoresistive elements are inherently linear. The elastic protective rubber, glued on the top of the membrane, acts as a separate information coding layer, changing the sensitivity and the spatiotemporal characteristics of the sensor [3], [4]. In order to characterize the effects of the elastic coating and the integral properties of the sensor, we carried out two different experiments. First, we measured the response to normal load attacking the center of the membrane (as in the previous case), then we investigated the spatially distributed response of the sensor by changing the position of the attacking point over the top surface.

Two elastic layers of different thickness were tested. The loads were applied through a $\varnothing$100-μm needle with forces in the range of 0–70 mN. The first sensor was covered with a 220-μm silicon rubber, which highly decreased the sensor's sensitivity, but did not change the linear characteristics.

The second sensor was covered with a thicker, 500-μm rubber layer (Fig. 9). The thicker rubber layer reduced the sensor's sensitivity even more—by around a factor of 30. Moreover, the force concentrated on the small region of the needle tip obviously resulted in a nonlinear behavior by the rubber, therefore creating an overall higher order exponential-like response.

C. Receptive Field Measurements

Sensors with an elastic layer on top react to loads applied not only to the center of the bridges but also outside the sensor area. Their receptive field (RF)[6] thus becomes extended. In this experiment, we tested these RFs with a constant load, normal

[6]The name comes from the analogous biological systems. Each mechanoreceptor in the deep layers of the human skin has a receptive field on the skin surface, denoting the area where that specific sensor can be activated.
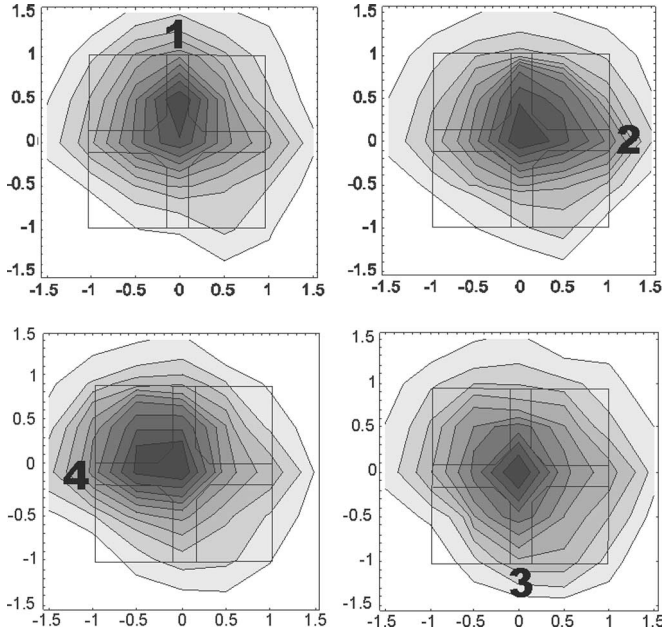
Fig. 10. Receptive field of the four bridges of a single taxel. Rubber thickness is 500 μm. The darker areas represent higher response. The position of the sensor is indicated in the response maps.

to the chip surface, moved across the rubber surface around the sensor. In the first experiment, we combined results from unique measurements to create an image of the two-dimensional (2-D) RFs (Fig. 10). The highest achieved spatial resolution of the positioning was 75 ± 20 μm in both spatial directions, therefore generating relatively low-precision data. The general shape and size of the RF, however, can be revealed by this method.

In the above arrangement, the taxel size is 300×300 μm^2, which corresponds to a sensitive area of around 500×500 μm^2. Since the spacing of the sensors in the test structure is 1.5 mm, we can provide overlapping RFs either by modifying the sensor coverage (i.e., changing the thickness and hardness of the rubber), or by increasing the resolution of the sensors in a close-packaged new design.

In order to gain information about the high-resolution shape of the RF, we used a second-type real-time measuring setup with the following experimental method: We positioned the loading tip to the exact center of the sensor and moved it across the surface in one direction—usually parallel to one sensor bridge—without lifting the load up from the rubber. This method had two advantages compared to the previous experiments: 1) visual feedback from real-time reconstruction of the measured force vectors minimized positioning error and 2) much higher spatial detail arose from the 30-ms scanning time.

Results on a sensor with 180-μm rubber on top can be seen in Fig. 11. To better catch the meaning of these curves, we have to convert the responses to the dimension of the strain components appearing at the sensor surface under the cover.

There is a method given in [2] for the reconstruction of the stress tensor elements from the four measured voltages of a bare four-bridge sensor. However, when an elastomer is present on top of the sensor, the stress arising at the Si surface is proportional to the strain distribution at the bottom of the elastic cover.
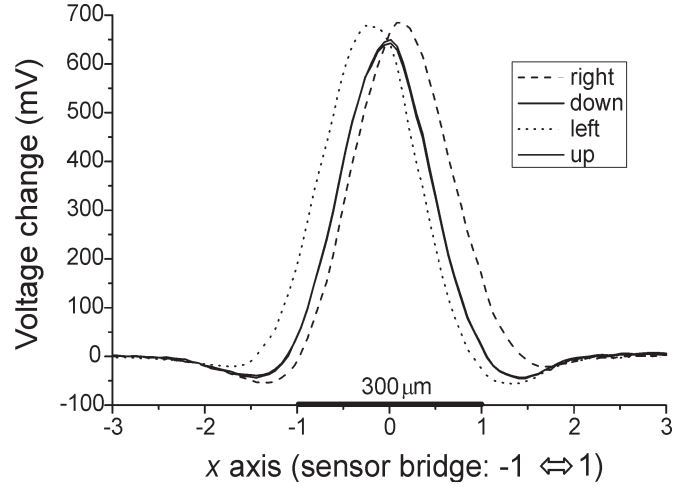

Fig. 11. One-dimensional (1-D) RF of a single taxel across the axis of one sensor bridge in the "left"–"right" direction. The four curves indicate the four piezoresistors. The "down" and "up" elements show perfect overlapping, as it is predicted by symmetry. Rubber thickness was 180 μm.

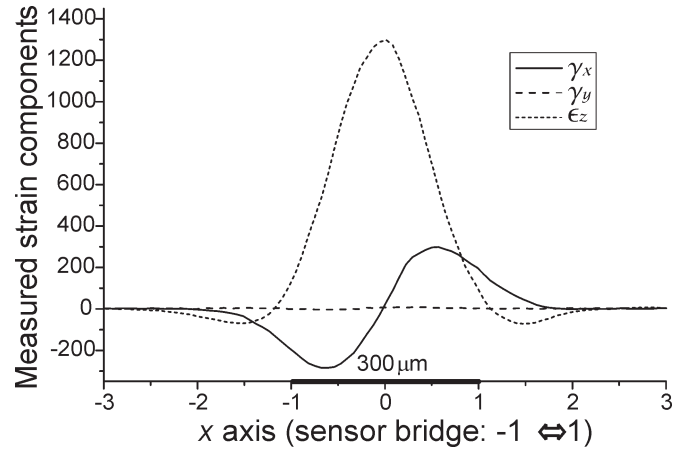

Fig. 12. Reconstructed, relative strain components under the elastic cover, assuming that $\alpha_s = \alpha_n = 1$/mV. γ_x and γ_x are the two shear components, ε_z is the normal strain. Sensor size and position is marked on the x-axis.

According to our experiments, the sensors, indeed, respond to the changes in the strain distribution in the rubber, not to those in the stress. In spite of this, the equations describing the connection between the measured voltages and the strain are similar to those in [2]:

$$\gamma_x = \alpha_s(\Delta V_{\text{left}} - \Delta V_{\text{right}})$$
$$\gamma_y = \alpha_s(\Delta V_{\text{down}} - \Delta V_{\text{up}})$$
$$\varepsilon_z = \frac{\alpha_n}{2}(\Delta V_{\text{left}} + \Delta V_{\text{right}} + \Delta V_{\text{down}} + \Delta V_{\text{up}}) \quad (3)$$

where γ_x, γ_y, and ε_z are the two shear and one normal-strain components, respectively, ΔV_i represents the measured voltage change, the α constants contain the piezoresistive coefficients and all the information about the geometry of the sensor and the amplification. The converted strain components of Fig. 11 can be seen in Fig. 12.

Results highly resemble to the curves derived from the semiinfinite continuum-mechanical model [7]. In this model, a point load is applied normally to an elastic half-space, and the
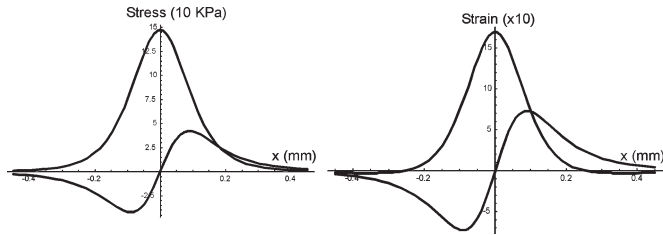
Fig. 13. Analytical results from the semiinfinite mechanical model, showing the stress and strain distribution under a point load. Parameters are set to match experimental data: Young-modulus is 0.87 MPa, Poisson's ratio is 0.5, applied force is 10 mN, solid thickness is 0.18 mm. Only the strain distribution has Mexican-hatlike characteristics, similar to that in our measurement.

stress and strain distribution inside the elastic solid is calculated analytically (Fig. 13). In the experiments, the tip diameter was 0.1 mm, therefore point loading is a good approximation.

The theoretical and experimental results show the same shape with the following exceptions.

1) Since our sensor surface is flat, it is less sensitive to shear forces. Shear sensitivity can be increased with the application of a rigid bump in the middle.
2) The measured response distribution is slightly narrower than the theoretical result with the appropriate parameters—it resembles more the analytical distribution in a thinner layer of rubber. As a visible consequence, our sensor shows strong lateral inhibition characteristics (Mexican-hatlike[7] distribution). It is interesting to note that in biological systems, the same center-surround effect appears in the mechanoreceptor's response (as a consequence of the mechanical properties of the skin) and it is used to increase the lateral spatial resolution of the neural signals [8], [9].

D. Membrane With Load Transmitting Rigid Plastic Rod Built on Top

Once a load-transmitting rod has been formed, the sensor reacts differently to tangential (shear) loads attacking from different directions. To measure shear load transmission, we still applied normal load but consecutively at different points, at a distance of 150 μm from the center. This way the tangential force is generated by the tangential deformation of the rubber opposite to the load [Fig. 14(a)]. The positioning error of the needle was again around $\pm$ 30 μm. Results are listed in Table II.

Again, we can use (3) to reconstruct the load components, as shown in Fig. 14(b).

In general, RF shapes are essentially modified by the application of the rigid bump. Sensors become highly sensitive to shear stress, while the sensitivity to the normal load is not affected. The ratio of the shear and the normal sensitivity can be set by choosing the proper size for the bump. With increasing the bump size, we also elongate the force arm for the membrane distortion, and thus shear sensitivity increases, too.
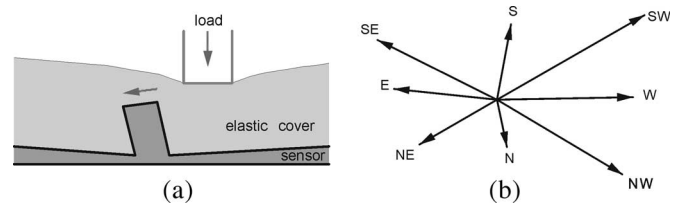

(a)   (b)

Fig. 14. (a) Measurement setup for determining response to shear forces. If the load is applied eccentrically, tangential forces arise. (b) Reconstructed force directions from the same measurement. If the normal load is applied on the left side (shown as West), the force direction points to the right. Differences in the force amplitudes are the results of the positioning error.

TABLE II
RESPONSE TO DIFFERENT TANGENTIAL LOADS, LABELED WITH THE RELATIVE POSITION OF THE INDENTATION FROM THE SENSOR CENTER. EACH ROW REPRESENTS ONE DIRECTION, EACH COLUMN REPRESENTS ONE BRIDGE. VALUES ARE IN (mV)

	1 (N)	2 (E)	3 (S)	4 (W)
N	6.2	−4.5	−14.5	−1.8
NE	5	3.3	−14.5	−17.1
E	−7.6	5.6	−2.8	−21.7
SE	−21.4	5.4	4.5	−26.2
S	−23.2	−6.3	9.4	−2.6
SW	−26.1	−24	10.5	15.1
W	−3.2	−21.4	−2.1	14.7
NW	11.8	−20.2	−20.6	13.1

V. CONCLUSION

A novel-type 3-D force-sensor design was proposed and manufactured for integrated tactile applications in robotic control. The monocrystalline Si piezoresistors are formed in suspended Si bridges using porous-silicon micromachining. The sensory elements provide optimum sensitivity, the 3-D decomposition of the attacking force and the possibility of integration with MOS circuits.

Accurate testing of the sensors is not straightforward. The shortcomings in the present loading equipment lead to the noise and asymmetries in the obtained results. The measurement error in the experiments is mainly due to the indefinite positioning of the load. However, in precise experiments sensor characteristics show almost perfect matching with theoretical results.

In tactile applications, overlapping RFs are required, as in analogous biological systems. It can be achieved by increasing taxel density and by tailoring the elastic properties of the load transferring protective layer.

Based on the presented results, a 64-element integrated sensor array will be formed to facilitate further research in biologically motivated robotic applications.

REFERENCES

[1] L. Wang and D. J. Beebe, "A silicon-based shear force sensor: Development and characterization," *Sens. Actuators*, vol. 84, no. 1, pp. 33–44, Aug. 2000.
[2] B. J. Kane, M. R. Cutkosky, and G. T. A. Kovacs, "A traction stress sensor array for use in high-resolution robotic tactile imaging," *J. Microelectromech. Syst.*, vol. 9, no. 4, pp. 425–434, Dec. 2000.
[3] R. S. Fearing and J. M. Hollerbach, "Basic solid mechanics for tactile sensing," *Int. J. Robot. Res.*, vol. 4, no. 3, pp. 40–54, Fall 1985.
[4] M. Shimojo, "Spatial filtering characteristic of elastic cover for tactile sensor," in *Proc. IEEE Int. Conf. Robot. and Autom.*, San Diego, CA, May 8–13, 1994, pp. 287–292.
[5] S. M. Sze, *Semiconductor Sensors*. New York: Wiley, 1994, p. 178.

---

[7]The real Mexican-hat distribution is the second derivative of the Gaussian function. In its simplest form it is as follows: $(1 - r^2) \exp\{-r^2/2\}$.

[6] Z. Vízváry, P. Fürjes, M. Ádám, C. Dücsõ, and I. Bársony, "Mechanical modeling of an integrable 3D force sensor by silicon micromachining," in *Proc. MME*, Sinaia, 2002, pp. 165–168.

[7] K. L. Johnson, *Contact Mechanics*. Cambridge, U.K.: Cambridge Univ. Press, 1985.

[8] J. R. Phillips and K. O. Johnson, "Tactile spatial resolution II. Neural representation of bars, edges, and gratings in monkey primary afferents," *J. Neurophysiol.*, vol. 46, no. 6, pp. 1192–1203, Dec. 1981.

[9] ——, "Tactile spatial resolution III. A continuum mechanics model of skin predicting mechanoreceptor responses to bars, edges, and gratings," *J. Neurophysiol.*, vol. 46, no. 6, pp. 1204–1225, Dec. 1981.

Zsolt Vízváry was born in Hungary in 1976. He received the M.Sc. degree in mechanical engineering from Technical University of Budapest, Budapest, Hungary, in 1999. He is currently working toward the Ph.D. degree and is going to defend his Ph.D. thesis in 2005 at the Technical University of Budapest.

Currently, he is a Lecturer at the Department of Applied Mechanics of the Budapest University of Technology and Economics, Budapest. His primary interests are the development finite-element method (FEM) methods for thermomechanical modeling of microstructures and characterization of materials applied in MEMS.

Gábor Vásárhelyi (S'05) was born in Budapest, Hungary, in 1979. He received the M.Sc. degree in engineering physics from Technical University of Budapest, Budapest, Hungary, in 2003. He is currently working toward the Ph.D. degree at Péter Pázmány Catholic University, Multidisciplinary Technical Sciences Doctoral School, Budapest.

Main research fields are tactile sensor arrays and tactile applications on cellular neural network (CNN) chips.

Attila Kis was born in Romania in 1977. He received the M.Sc. degree in electrical engineering from Technical University of Tirgu Mures, Romania, in 2001. He is currently working toward the Ph.D. degree at Péter Pázmány Catholic University, Multidisciplinary Technical Sciences Doctoral School, Budapest, Hungary.

From 2001 to 2002, he was Coresearcher at the Computer and Automation Research Institute of the Hungarian Academy of Sciences, Analogical and Neural Computing Systems Laboratory. His research interests are biologically inspired real-time information processing on tactile sensor arrays, wave computing, cellular nonlinear network universal machine (CNN-UM), autonomous robots, integrated tactile and vision systems, and smart sensors.

Mária Ádám was born in Hungary in 1948. She received the M.Sc. degree in electrical engineering from the Technical University of Budapest, Budapest, Hungary, in 1973.

She was R&D Engineer at Tungsram Ltd., at the Department of Semiconductors, from 1973 to 1982. From 1982–1985, she spent three years with the Microelectronics Co. Currently, she is a Research Engineer at the Microelectromechanical Systems (MEMS) Laboratory of the Research Institute for Technical Physics and Materials Science (MFA). Her research interests include design, development and processing of silicon-based mechanical, and gas microsensor structures. She is coauthor of about 25 scientific papers and one patent.

István Bársony (M'97) was born in Hungary in 1949. He received the Dipl. Ing. degree in microelectronics from the Technische Hockschule Ilmenau, Ilmenau, Germany, in 1971 and the Ph.D. and D.Sc. degrees in microelectronics from the Hungarian Academy of Sciences and Technical University of Budapest.

Currently, he is the Director of MFA, Budapest, Hungary, and Professor of nanotechnology at the University of Veszprém, Hungary. His research interests are Si microtechnology, MEMS, and nanotechnology. He authored and coauthored over 100 scientific papers and holds 13 patents.

Éva Vázsonyi was born in Hungary in 1941. She received the M.Sc. degree in chemical engineering from Technical University of Budapest, Budapest, Hungary, in 1965.

She worked for the Tungsram Ltd. at the Department of Semiconductors and later joined the Technical University as a Research Fellow. In 1972, she joined the Central Research Institute for Physics and currently she works for one of its successor, the MEMS Laboratory MFA. Her research interests include fine line lithography and silicon micromachining. She has four patents, and is author and coauthor of about 60 scientific papers.

Csaba Dücsõ was born in Hungary in 1959. He graduated as a chemist in 1983 and received the Ph.D. degree in chemistry from Lóránd Eötvös University, Budapest, Hungary.

Currently, he is the Head of the MEMS laboratory of MFA, Budapest, Hungary. His research interests include Si-based MEMS with special emphasis on integrated gas and mechanical sensors and the development of the related processing technology. He is coauthor of over 50 papers published in periodicals and conference proceedings.